Article

pubs.acs.org/Biomac

MRI-Visible Poly(ε-caprolactone) with Controlled Contrast Agent Ratios for Enhanced Visualization in Temporary Imaging Applications

Sarah El Habnouni, Benjamin Nottelet,* Vincent Darcos, Barbara Porsio, Laurent Lemaire,† Florence Franconi,‡ Xavier Garric, and Jean Coudane

Institut des Biomolécules Max Mousseron (IBMM), UMR CNRS 5247, University of Montpellier 1, University of Montpellier 2 − ENSCM, Faculty of Pharmacy, 15 Av. C. Flahault, Montpellier, 34093, France

†Micro et Nanomédecines Biomimétiques (MINT), UMR-S 1066, Université d'Angers, 4 rue Larrey, 49933 Angers Cedex9, France

‡PIAM, UFR Sciences, 2bd Lavoisier, 49045 Angers, France

Supporting Information

ABSTRACT: Hydrophobic macromolecular contrast agents (MMCAs) are highly desirable to provide safe and efficient magnetic resonance (MR) visibility to implantable medical devices. In this study, we report on the synthesis and evaluation of novel biodegradable poly(ε-caprolactone)-based MMCAs. Poly(α-propargyl-ε-caprolactone-*co*-ε-caprolactone)s containing 2, 5, and 10 mol % of propargyl groups have been prepared by ring-opening copolymerization of ε-caprolactone and the corresponding propargylated lactone. In parallel, a diazido derivative of the clinically used diethylenetriaminepentaacetic acid (DTPA)/Gd^{3+} complex has been synthesized. Finally, MRI-visible poly(ε-caprolactone)s (PCLs) were obtained by the efficient click ligation of these compounds via a Cu^{I}-catalyzed [3 + 2] cycloaddition. ICP-MS analyses confirmed the efficient coupling of the complex on the PCL backbone with the MRI-visible PCLs containing 1.0, 2.6, and 3.6 wt % of Gd^{3+}. The influence of the Gd^{3+} grafting density on the T_1 relaxation times and on the MRI visibility of the novel biodegradable MMCAs was evaluated. Finally, their stability and cytocompatibility were assessed with regard to their potential as innovative MRI-visible biomaterials for biomedical applications.

INTRODUCTION

Magnetic resonance imaging (MRI) is today one of the noninvasive technique of choice to provide high spatial and temporal resolutions in clinical diagnosis and staging of human diseases.[1] Unfortunately, in the case of polymeric prostheses there is an inability to provide a postoperative image of implanted prostheses, as polymeric biomaterials are intrinsically transparent to X-rays and are invisible using clinical MRI.[2,3] In some cases, the signal void of the prosthetic material can be useful for diagnoses, however it strongly depends on the size of the prostheses and on the site of implantation. Therefore this inability to visualize implanted material restricts the evaluation of the tissue integration, the postoperative fixation and the material's fate in the body.[4] This led us to consider in the past the possibility to produce radio-opaque degradable polyesters. A first example was provided by the radio-opaque poly(ε-caprolactone) (PCL) obtained by the anionic chemical modification of PCL with iodine to generate a poly(α-iodo-ε-caprolactone-*co*-ε-caprolactone) copolymer.[5] More recently, this postmodification strategy was applied to the synthesis of MRI-visible PCL and MRI-visible poly(methyl acrylate) (PMA) that were among the first examples of hydrophobic MRI-visible thermoplastics.[6,7] Indeed, although MRI polymers have attracted much attention in the recent past, most efforts are dedicated to water-soluble polycondensate or amphiphilic structures to be used in drug delivery approaches.[8−17] In particular, a preferred strategy relies on the modification of diblock amphiphilic copolymers with a contrast agent to yield macromolecular contrast agents (MMCAs) able to self-assemble into micellar systems.[13,18−22] These water-soluble MMCAs are rapidly excreted and cannot be used for the MRI visualization of non water-soluble implanted devices. Another strategy relies in the development of nonclassical MRI techniques, as exemplified by the recent use of amide proton transfer MRI technique to visualize hydrophilic and fast resorbing collagen coatings.[23] In this regard, the originality of the postmodification approach used by our group lies in the possibility of providing hydrophobic and multivalent MMCAs. However, one limitation was the lack of fine control over the final substitution degree of the polymeric backbone and the necessity to use protection/deprotection steps to covalently bind the ligand diethylenetriaminepentaacetic acid (DTPA) before final complexation of the Gd^{3+} MRI contrast agent. Yet, control of the overall amount of contrast agent, as well as its repartition along the polymer chain and its chemical environment, are known to influence the resulting relaxivity and visualization.[24] The strategy chosen in this work to prepare hydrophobic and multivalent MMCAs addresses these points. It is based on the convergent synthesis of an azide-containing contrast agent, and of a propargyl-functionalized PCL whose late ligation occurs via Cu^{I}-catalyzed [3 + 2] cycloaddition reaction. Practically, the control of the functionalization of

Received: July 5, 2013
Revised: September 4, 2013
Published: September 5, 2013

propargylated PCLs is conveniently obtained by ROP of εCL and αPgεCL, as recently described by our group,[25] whereas the use of a click chemistry reaction for ligation ensures a quantitative functionalization of the polymer by the contrast agent. Finally, the direct coupling of the Gd^{3+} complex on the polymer avoids the late complexation step between the macromolecular ligand and Gd^{3+}, which is generally of lower efficiency to control the final amount of immobilized contrast agent.[7]

We thus propose in this work a so far nonexplored strategy for the efficient and controlled Gd^{3+}-functionalization of aliphatic degradable polyesters to provide biocompatible and slow degrading hydrophobic MRI-visible thermoplastics for long-term MR visualization. Synthesis of copolyesters MMCAs with finely controlled compositions is described. The influence of the copolymers nature is discussed with respect to their MR visualization. Finally, stability of these MMCAs and their cytocompatibility are assessed.

EXPERIMENTAL SECTION

Materials. Isopropanol, ε-caprolactone, and toluene were dried over calcium hydride for 24 h at room temperature and distilled under reduced pressure. Tetrahydrofuran was dried by refluxing over a benzophenone-sodium mixture and distilled. All other materials were obtained from Aldrich and were used without further purification.

NMR Spectroscopy. ^1H and ^{13}C NMR spectra were recorded on a Bruker spectrometer (AMX300) operating at 300 and 75 MHz, respectively. Deuterated chloroform or deuterated dimethyl sulfoxide were used as solvents. Chemical shifts were expressed in ppm with respect to tetramethylsilane (TMS).

Relaxation times for polymers dissolved in DMSO-d_6 were measured on an AMX400 Bruker spectrometer operating at 400 MHz. T_1 measurements were obtained using T_1 inversion/recovery sequence. Analyses were carried out at 80 °C to facilitate the molecular mobility of the polymer. A fixed concentration of 11 mg/mL was used for all samples.

FT-IR Spectroscopy. Infrared spectra were recorded on a Perkin-Elmer Spectrum 100 FT-IR spectrometer using the attenuated total reflectance (ATR) method.

LC-MS Analyses. LC/MS analyses were performed on a Q-TOF (Waters) spectrometer fitted with an electrospray interface. Solvent used for HPLC and LC/MS were HPLC grade. MALDI analyses were performed on a Ultra-Flex III (Bruker) spectrometer using a dithranol matrix.

Size Exclusion Chromatography. Size exclusion chromatography (SEC) was performed at room temperature on a Waters system equipped with a guard column, a 600 mm PLgel 5 mm Mixed C column (Polymer Laboratories), and a Waters 410 refractometric detector. Calibration was established with poly(styrene) standards from Polymer Laboratories. THF was used as eluent at a flow rate of 1 mL/min.

ICP-MS Analyses. Gd^{3+} was quantified using an Element XR sector field ICP-MS (inductively coupled plasma-mass spectrometry) at Géosciences in Montpellier (University Montpellier II). Internal standardization used an ultrapure solution enriched with indium.

Synthesis and Characterization of MRI-Visible PCL. *Synthesis of Diazido Functionalized Diethylenetriaminepentaacetic Acid (diN_3-DTPA) **1**.* In a first step, 1-azido-3-aminopropane was prepared according to a previously described procedure.[26] A solution of 3-chloropropylamine hydrochloride (4 g; 30.8 mmol) and sodium azide (6 g; 92.3 mmol) in water (1 mL per mmol) was heated at 80 °C overnight. After removing most of the water by distillation under vacuum, the reaction mixture was cooled in an ice bath. Diethyl ether (50 mL) and KOH pellets (4 g) were added, keeping the temperature below 10 °C in an ice bath. After separation of the organic phase, the aqueous layer was further extracted with diethyl ether (2 × 20 mL). The combined organic layers were dried over $MgSO_4$ and concentrated to give oil which was purified by distillation. Colorless oil (2.46 g) was obtained (80% yield; Figure S1). RMN ^1H (300 MHz, $CDCl_3$) δ (ppm): 3.33 (t, 2H, CH_2N_3), 2.55 (t, 2H, CH_2NH_2), 2.34 (s, 2H, NH_2), 1.55 (q, 2H, $CH_2CH_2CH_2$). FT-IR (ATR, cm^{-1}): 2100 (N_3).

In a second step, diN_3-DTPA was synthesized according to a modified described procedure.[27] Typically, 1-azido-3-aminopropane (0.616 g; 6.2 mmol) was reacted with DTPA dianhydride (1 g; 2.8 mmol) in anhydrous DMF (20 mL) at room temperature and under nitrogen for 24 h. DMF was distilled under vacuum until 2−3 mL in volume and precipitated into diethyl ether. The obtained solid was further dissolved in water and lyophilized to yield a white solid (1.48 g, 95% yield). RMN ^1H (300 MHz, DMSO) δ (ppm): 3.4 (6H, CH_2CO_2H), 3.1 (12H, $N(CH_2)_2N$ and $NCH_2C(O)$), 2.8 (8H, $CH_2NHC(O)$ and CH_2N_3), 1.7 (4H, $CH_2CH_2N_3$). FT-IR (ATR, cm^{-1}): 2100 (N_3). LC-MS (ES+, *m/z*): 558.4 Da $[M + H^+]$.

Caution: ω-aminoalkyl azides being potentially explosives all reactions involving this compound were carried out with the appropriate protection under a well ventilated hood.

*Preparation of Clickable Gd^{3+} Complex **2**.* Pyridine (1.44 mL; 17.9 mmol) was added to an aqueous solution of **1** (1 g; 1.79 mmol). After 10 min stirring at room temperature a clear solution was obtained and $GdCl_3{\cdot}6H_2O$ (1.33 g; 3.58 mmol) was added. Complexation was let to run under stirring at 40 °C for 24 h. Water and pyridine were removed by distillation under vacuum. The resulting solid was dissolved in water before purification on a Chelex 100 resin. After lyophylization **2** was obtained as a white solid (90% yield). Absence of free Gd^{3+} was confirmed by a methyl thymol blue (MTB) test[28] (Figure S2), whereas the content of complexed Gd^{3+} in **2** was quantitatively determined by ICP-MS. FT-IR (ATR, cm^{-1}): 2100 (N3). MALDI-TOF (dithranol *m/z*): $[M + H]^+$ *m/z* 713.16 Da; $[2M + H]^+$ *m/z* calcd, 1423.33 Da; theoretical, 713.17 and 1425.34. Gd^{3+} content (ICP-MS): 15.4 wt %.

*Synthesis of Poly(α-propargyl-ε-caprolactone-co-ε-caprolactone)s P(Pg-CL) **3**.* α-Propargyl-ε-caprolactone (αPgεCL) was synthesized from εCL by an anionic modification approach already described elsewhere.[25] Polymerization was carried out in bulk using standard Schlenk technique under an inert atmosphere of argon. Amounts of εCL and αPgεCL were added in the reaction flask according to the targeted compositions. In a typical experiment, εCL (2.66 g; 29.6 mmol), αPgεCL (0.5 g; 3.29 mmol), $Sn(Oct)_2$ (66.4 mg; 0.164 mol), and isopropanol (25 μL; 0.328 mmol) were placed in an oven-dried Schlenk tube. The tube was fitted with a rubber septum. The solution was further degassed by three freeze−pump−thaw cycles. The resulting mixture was stirred at 140 °C for 3.5 h. To stop the reaction, polymerization was quenched by addition of an excess of 1 N HCl. The reaction mixture was poured into cold methanol. The precipated polymer **3** was collected by filtration and dried in vacuum. ^1H NMR (300 MHz, $CDCl_3$) δ (ppm): 4.96 (m, $(CH_3)_2CH$), 4.02 (t, CH_2O), 3.60 (m, CH_2OH), 2.50 (m, $COCHCH_2$), 2.26 (t, $COCH_2$), 1.96 (m, $C{\equiv}CH$), 1.49−1.70 (m, CH_2-CH_2-CH_2-CH_2-O-), 1.29−1.42 (m, m, CH_2-CH_2-CH_2-CH_2-O-), 1.18 (d, $(CH_3)_2CH$). IR (ATR, cm^{-1}): 3280 (C≡CH), 1720 (C═O). Mn_{SEC} = 18000 g/mol, $Đ$ = 1.7.

*Synthesis of MRI-Visible Poly(ε-caprolactone)s (MRI-PCLs) **4**.* Copolymer **3**, complex **2** (3 equiv/αPgεCL units) and CuBr (2 equiv/αPgεCL units) were solubilized in DMF. The solution was degassed by three freeze−pump−thaw cycles. *N,N,N′,N″,N″*-Pentamethyldiethylenetriamine (PMDETA) (2 equiv/ αPgεCL units) degassed by argon bubbling was added to the reaction medium. The reaction was carried out for 48 h at room temperature under stirring. The crude medium was dissolved in THF for dialysis (MWCO 3500 g/mol) against distilled water. Copolymer **4** was recovered after removal of the solvents and drying in vacuum. Copolymers with 1.0, 2.6, and 3.6 wt % of Gd^{3+}, as determined by ICP-MS, were noted $\mathbf{4_1}$, $\mathbf{4_2}$, and $\mathbf{4_3}$, respectively.

MRI Visualization. *MR Imaging Protocol.* MR imaging experiments were performed on a Bruker Avance DRX system (Bruker Biospin SA, Wissembourg, France). The system was equipped with a 150 mm vertical superwide-bore magnet operating at 7 T, a 84 mm inner diameter shielded gradient set capable of 144 $mT{\cdot}m^{-1}$ maximum gradient strength and a 30 mm diameter birdcage resonator. Modified

Scheme 1. Reaction Scheme for the Synthesis of MRI-PCLs 4[a]

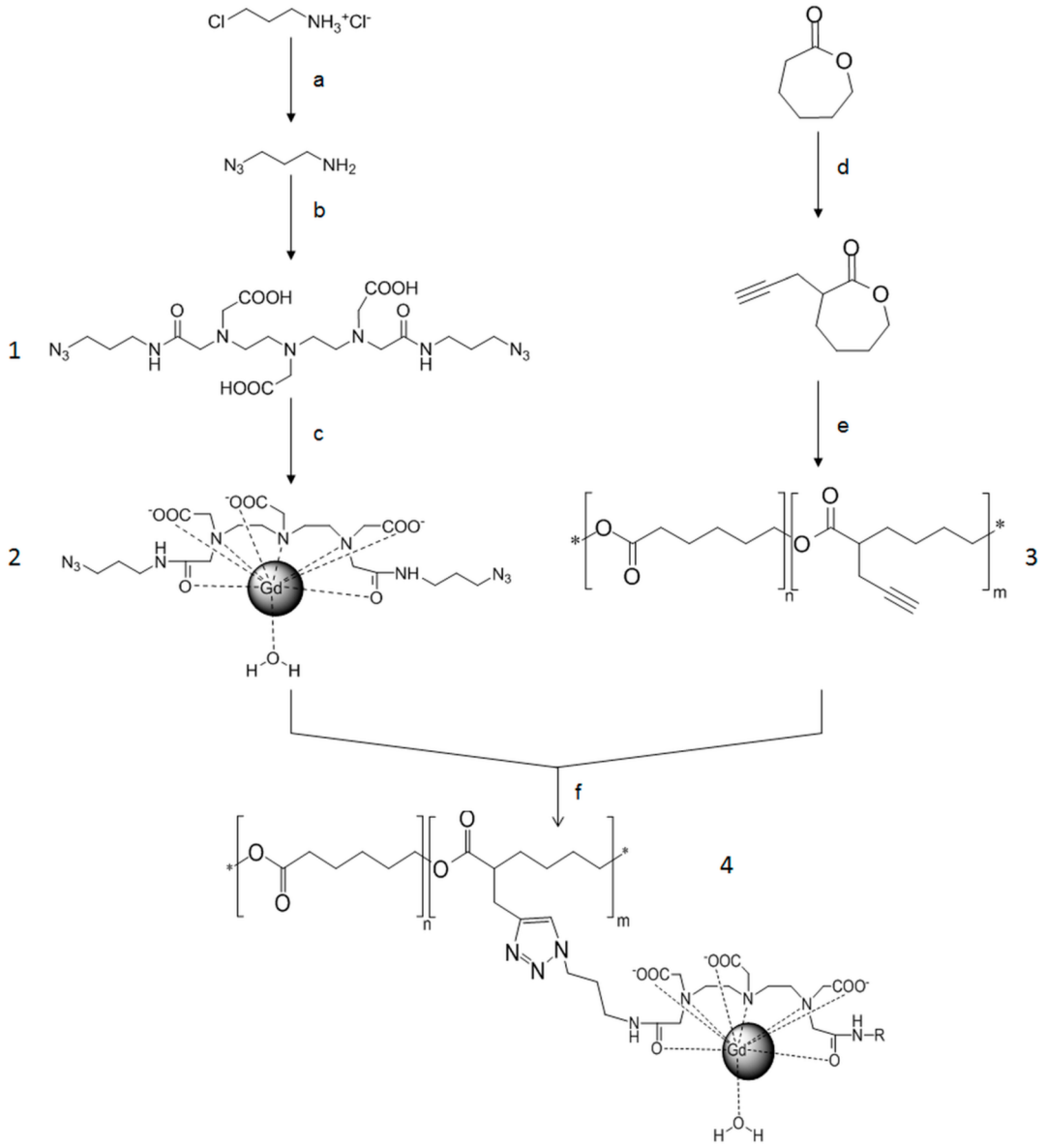

[a]Reagents and conditions: (a) NaN_3, water, 80 °C, overnight; (b) DTPA dianhydride, DMF_{an}, RT, 24 h; (c) pyridine, RT, 10 min/$GdCl_3 \cdot 6H_2O$, 40 °C, 24 h; (d) LDA, THF_{an}, −78 °C, 1 h/propargyl bromide, THF_{an}, −30 °C, 3 h; (e) εCL, $Sn(Oct)_2$, iPrOH, 140 °C, 3.5 h; (f) CuBr, PMDETA, DMF, RT, 48 h.

or native PCL films (~1 cm^2) were embedded in a degassed 1% (w/w) agarose gel prior to imaging. Gadolinium-free samples corresponded to a PCL film. To test signal enhancement, T_1 weighting was introduced into the MR images using an inversion pulse[29] in rapid three-dimensional (3-D) acquisition with relaxation enhancement (RARE) sequence (TR = 3000 ms; mean echo time (TEm) = 8 ms; RARE factor = 8; FOV = 3 × 3 × 1.5 cm; matrix 128 × 128 × 64). Inversion time was set at 1100 ms, sufficient to allow canceling of the embedding gel.

Stability Studies. MRI-visible films were prepared with high (0.4 wt %) and low (0.1 wt %) contents of Gd^{3+}. Films were prepared by dissolution of the appropriate amounts of PCL and $\mathbf{4_2}$ in dichloromethane followed by solvent evaporation. Film samples (10 mg) were cut out for stability studies. Released gadolinium was quantified by ICP-MS after sample immersion in 10 mL of PBS saline buffer and stirring at 130 rpm and at 37 °C. At scheduled time points (1, 3, 7, 15, 30, and 90 days), 1 mL aliquots of solution were taken and replaced by fresh buffer. Gd^{3+} was quantified by ICP-MS.

In Vitro Cytocompatibility. Murine fibroblasts cells (designated L929) were used to assess the in vitro cytocompatibility of the materials as recommended by the International and European Standards (ISO 10993−5:2009). L929 cells were cultured in DMEMα supplemented with 10% fetal bovine serum (FBS), penicillin (100 U/mL), streptomycin (100 μg/mL), and glutamine (2 mM). Sample disks (ø 15 mm) were cut from copolymer films and disinfected in ethanol for 30 min before immersion in a solution of sterile PBS containing penicillin and streptomycin (1 mg/mL) and incubation for 48 h at 37 °C. Films were then rinsed 2 times with sterile PBS before soaking for 12 h in sterile PBS. After disinfection, disks were placed in TCPS 12-well plates and Viton O-rings were used to maintain the samples on the bottom of the wells and avoid cells growing on TCPS underneath the samples. Disks were finally seeded with 1 × 10^4 cells and viability was evaluated after 1, 2, and 3 days using PrestoBlue assay, which reflects the number of living cells present on a surface at a given time point. At scheduled time points, culture medium was removed and replaced by 1 mL of fresh medium

Table 1. Properties of P(Pg-CL)s 3 and MRI-PCLs 4

P(Pg-CL)s				MRI-PCLs				
	$F_{\alpha PreCL}$	$\bar{M}_n$ SEC[a] (g/mol)	$Đ$		Gd wt% single ligation (calculated)	Gd wt% cross-linking (calculated)	Gd wt%[b] (experimental)	Gd mol%[c] (experimental)
P(Pg-CL)$_2$ **3$_1$**	2	34000	2.3	P(DPTA[Gd]-CL)$_2$ **4$_1$**	2.4	1.2	1.0	0.8
P(Pg-CL)$_5$ **3$_2$**	5	25000	1.9	P(DPTA[Gd]-CL)$_5$ **4$_2$**	5.4	2.7	2.6	2.1
P(Pg-CL)$_{10}$ **3$_3$**	10	18000	1.7	P(DPTA[Gd]-CL)$_{10}$ **4$_3$**	8.6	4.3	3.6	3.0

[a]SEC analyses with THF as solvent and PS standards. [b]Determined by ICP-MS. [c]Calculated from the weight percentages.

containing 10% of PrestoBlue. After 2 h of incubation at 37 °C, 200 μL of supernatant were taken from each well and analyzed for fluorescence at 530 nm (ex.) and 615 nm (em.) with a Victor X3 (Perkin-Elmer).

RESULTS AND DISCUSSION

Synthesis of MRI-Visible Poly(ε-caprolactone)s (MRI-PCLs). *Preparation of Clickable Gd^{3+} Complex 2.* The present work aims at providing MRI-PCLs with controlled content of gadolinium by coupling of an azide-containing contrast agent to a propargyl-functionalized PCL obtained by ROP of εCL and αPgεCL. In this regard, the first step consisted in the preparation of diazido functionalized diethylenetriaminepentaacetic acid (diN_3-DTPA; Scheme 1). Our choice to use a bifunctional ligand was motivated by scale-up considerations with regard to the final context of biomaterials where multigram scale MRI-PCLs would be required. Indeed, although described in the literature, the synthesis of monofunctional DOTA-, DTTA-, or DTPA-based ligands is a multistep process that requires careful purifications.[30−33] Commercially monofunctional ligands are also available but, due to the mentioned synthetic problems encountered, they still are specialty chemicals whose expensive costs are limiting their use to applications where very low functionalizations are required, like for example in the case of polymer monosubstitution.[19] We thus preferred to base our approach on a straightforward and cost-effective preparation of diN_3-DTPA. As will be discussed in In Vitro Stability of MRI-PCLs, although difunctional ligands possess less coordinating groups, the use of such a ligand was not detrimental to the overall complex stability. A similar approach was already used by Perez-Baena et al.[27] who prepared dipropargyl-DTPA for cross-linking reactions of polyacrylic derivatives. In the present work, compound **1** was readily synthesized from commercially available DTPA dianhydride and an excess of 1-azido-3-aminopropane, by an amidification reaction in almost quantitative yield. No monofunctional derivative was produced under the chosen conditions as proved by the single peak at 558.4 Da [M + H$^+$] obtained in LC-MS analysis (data not shown) in accordance with the theoretical value of 558.3 Da. The formation of the desired diazide was further corroborated by ^{1}H NMR and FT-IR analyses (Figure S1). The subsequent complexation of **1** with $GdCl_3{\cdot}6H_2O$ yielded chelate **2** in good yield. Purification on Chelex 100 resin was used to efficiently remove the noncomplexed Gd^{3+}. The absence of free Gd^{3+} was confirmed by a methyl thymol blue (MTB) test (λ_{ABS} max = 425 nm; Figure S2). MALDI-TOF analysis showed three peaks corresponding to residual free chelator **1** at 558.2 Da and the protonated complex **2** under a monomeric form (713.2 Da) and a dimeric form (1423.3 Da) resulting from shared electrostatic interactions between two complexes **2**. ICP-MS analysis showed a 70% complexation ratio of Gd^{3+} with **1**. It should be noted that complexation conditions vary in literature depending on the chelate. Classically, temperature and reaction time are used to optimize complexation. In this work, higher temperatures could not be used to guarantee the conservation of the thermo-labile azide groups, and complexation time was doubled without benefice. However, it is well-known that commercial contrast agents like Magnevist, which chelating agent is DTPA, contain non complexed ligands (ca. 2%) to ensure the chelation of potentially released free Gd^{3+}.[34] One may wonder the potential biological effect of the 30% remaining free chelate, especially with regard to a potential complexation of calcium in vivo. This point will be addressed in the last paragraph regarding biocompatibility.

Synthesis of MRI-Visible Poly(ε-caprolactone)s (MRI-PCLs) 4. In parallel to the synthesis of **2**, propargylated PCLs (P(Pg-CL)) **3** were prepared. This was achieved by the copolymerization of αPgεCL and εCL, as already described by our group.[25] ROP allowed generating a family of copolymers with a controlled ratio of propargylated units whose properties are summarized in Table 1. Quantitative incorporation of the propargylated units was obtained. Polymers were characterized by NMR, SEC, and FT-IR. Increased intensities of the signals characteristic of the propargyl group at 1.96 ppm on the NMR spectra and at 3300 cm^{-1} on the FT-IR spectra were observed (Figures S3−S5). Our aim being to study the influence of the contrast agent grafting density on the polymer visualization, three copolymers were prepared with 2, 5, and 10% of propargyl units (**3$_1$**, **3$_2$**, and **3$_3$**, respectively). We limited our study to low ratios because our previous work on MRI-visible PCLs proved the efficient visualization of polymers incorporating low amounts of contrast agents.[6]

MRI-PCLs **4** were finally obtained by a Cu^I-catalyzed [3 + 2] cycloaddition between the azide groups of **2** and the alkyne groups of **3**. Typically, a 3 equiv excess of **2** relative to the alkyne moles present in copolymers **3** was used and reaction was performed in a dilute regime to avoid nondesired intermolecular cross-linking and to favor the reaction of **2** with a single propargyl group (Scheme 2). Under these conditions, complex **2** was efficiently coupled to P(Pg-CL) copolymers **3** via 1,2,3-triazole groups without precipitation of the resulting polymer that remained soluble in the reaction medium. Compounds **4** were first characterized by NMR and FT-IR. FT-IR spectra showed bands at 1690 cm^{-1} corresponding to the carboxylate groups engaged in the complexation of Gd^{3+}. Bands at 2100 cm^{-1} corresponding to residual free azide groups were also visible (Figure 1), thus, confirming that part of ligands **2** reacted with a single propargyl group (Scheme 2a). ^{1}H NMR experiments showed the expected peaks of PCL with a strong perturbation of the proton signal that increased with the content of immobilized contrast agent on the polymer backbone (Figure 2). As expected, peak broadening was observed as a consequence of the perturbation induced by

Scheme 2. Possible Structures of MRI-PCLs 4 as a Function of the Type of Ligation[a]

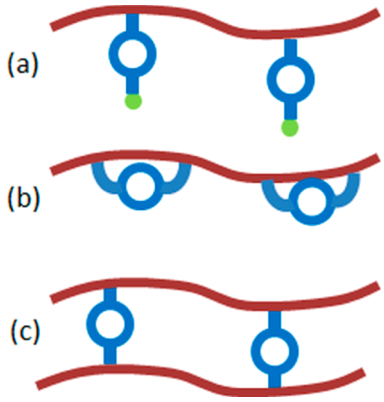

[a](a) Single ligation, (b) intramolecular crosslinking, and (c) intermolecular crosslinking (in brown: PCL backbone, in blue: ligand **2**, in green: free azide groups).

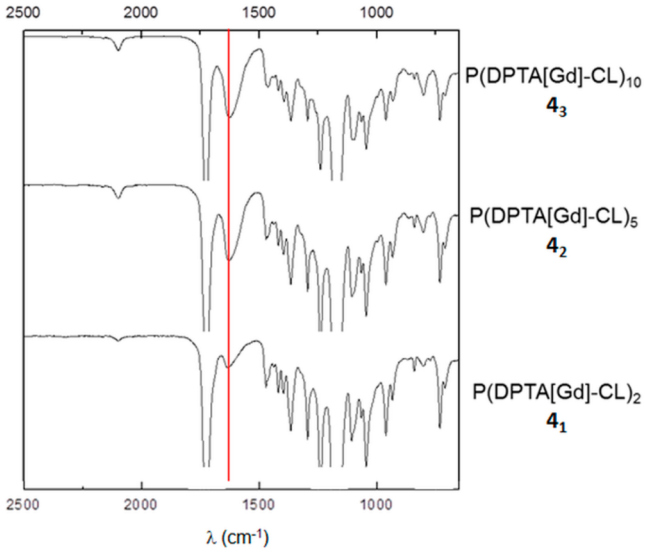

Figure 1. FT-IR spectra of MRI-PCLs copolymers $\mathbf{4}_{1-3}$. The plain line highlights the band at 1690 cm^{-1} corresponding to the carboxylate groups engaged in the complexation of Gd^{3+}.

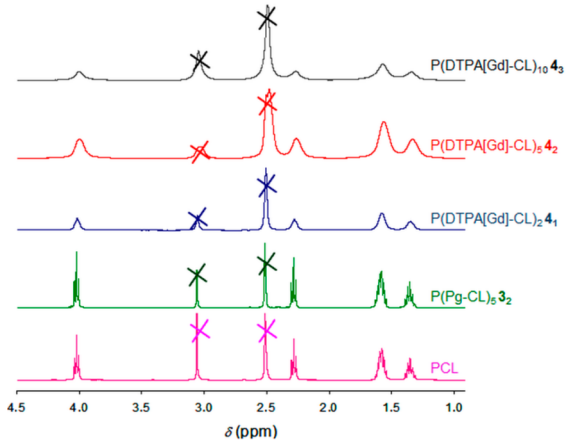

Figure 2. ^{1}H NMR (DMSO-d_6, 300 MHz) spectra of PCL, P(Pg-CL) $\mathbf{3}_2$, and MRI-PCLs copolymers $\mathbf{4}_{1-3}$ (marks correspond to DMSO-d_6 at 2.5 ppm and residual water at 3.3 ppm).

Gd^{3+}, and no quantification could be done by NMR. A MTB test was performed after decomplexation of Gd^{3+} by treatment of MRI-PCLs in nitric acid to obtain a qualitative visualization of the amount of Gd^{3+} present in the macromolecular contrast agents (Figure S6). To quantitatively characterize the MRI-PCLs, ICP-MS analyses were performed. Results are listed in Table 1 and can be used to determine the type of ligation, that is, single ligation, intra-, or intermolecular cross-linking. Indeed, two ideal cases can be considered with either only the single ligation occurring (Scheme 2a) or only double ligations, that is, intra- or intermolecular cross-linking taking place (Scheme 2b,c). The expected weight percentages of Gd^{3+} should be twice higher in the first case compared to the second one. Calculated values of these two ideal scenarios are provided in Table 1. Results show a good agreement between the experimental amounts of Gd^{3+} found and the values calculated when considering only intra- or intermolecular cross-linking. Starting from copolymers $\mathbf{3}_1$, $\mathbf{3}_2$, and $\mathbf{3}_3$, containing 2, 5, and 10% of alkyne groups, respectively, the weight percentages of complexed gadolinium obtained were 1.0, 2.6, and 3.6 wt %, to be compared with theoretical values of 1.2, 2.7, and 4.3 wt %, respectively. These results, combined to the free azido groups shown by FT-IR analysis and the maintained solubility of the copolymers **4**, tend to demonstrate that the intramolecular cross-linking scenario shown in Scheme 2b is predominant in our system with only a limited amount of **2** reacting via a single ligation. The concordance between the calculated and the experimental values also proves the soundness of the chosen strategy based on the use of complex rather than on the postcomplexation of Gd^{3+} with a PCL macroligand. Indeed, this strategy enabled the efficient coupling of contrast agents on the degradable PCL backbones without decomplexation of gadolinium from **2** during the coupling reaction, which yields MRI-visible PLCs with predetermined amounts of Gd^{3+}.

MR Characterizations. *MRI-PCLS T_1 Relaxation Time Measurements.* The effect of grafted gadolinium was measured by determining the T_1 relaxation time for hydrogen atoms on the MRI-PCLs backbone. As expected, the longitudinal relaxation time T_1 of hydrogen atoms on MRI-PCLs was significantly lower than in genuine PCL (Table 2). As observed

Table 2. Longitudinal Relaxation Times T_1 of PCL and Compounds $\mathbf{3}_2$ and $\mathbf{4}_{1-3}$[a]

		T_1 relaxation time (ms)				
proton	δ (ppm)	PCL	$\mathbf{3}_2$	$\mathbf{4}_1$	$\mathbf{4}_2$	$\mathbf{4}_3$
A	4.0	1554	1558	536	273	252
B	2.3	1587	1694	562	289	346
C	1.3	1514	1505	554	291	196
D	1.4	1512	1502	552	299	289

[a]400 MHz, DMSO-d_6, 80 °C, 11 mg/mL.

in our previous study,[6] T_1 decreased with Gd^{3+} substitution ratio, and all protons of the MRI-PCLs were similarly impacted. At this point, one can note that, although not obtained by the same chemical strategies, T_1 relaxation times were comparable to the ones obtained by Blanquer et al.[6] Typically, for the reported PCL containing 0.8 wt % of Gd^{3+} a relaxation time of about 600 ms was found. This matches the 550 ms found for $\mathbf{4}_1$ containing 1.0 wt % of Gd^{3+}. Advantageously, the chemical strategy reported here allows the targeting of defined Gd^{3+} contents. As a consequence, it is possible to precisely evaluate the relative decrease of T_1 relaxation time for the protons of

dx.doi.org/10.1021/bm400978a | Biomacromolecules 2013, 14, 3626−3634

compounds **4** compared to genuine PCL as a function of their gadolinium content. This is shown in Figure 3. To clarify the

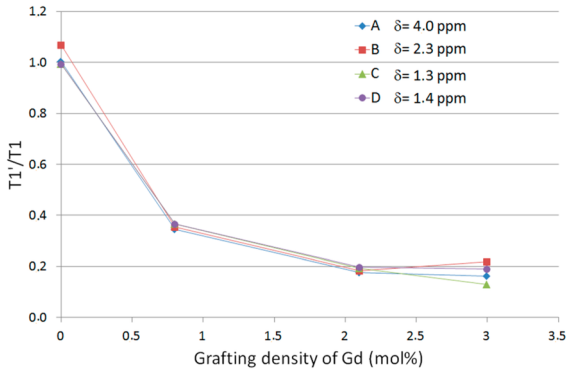

Figure 3. Influence of the grafting density of gadolinium on the T_1 relaxation time of MRI-PCLs protons (T_1' and T_1 are the T_1 relaxation times of compounds **4** and genuine PCL, respectively).

discussion, grafting densities, that is, molar percentages of CL units substituted by Gd^{3+}, have been calculated based on the experimental values of Gd^{3+} weight percentages (Table 1) and used in Figure 3. Two main observations can be drawn from this nonlinear evolution. First, it is noticeable that T_1 relaxation times are strongly influenced even when low grafting densities of Gd^{3+} are found on the polymers backbone, as shown by the 70% decrease of T_1 in copolymer $\mathbf{4_1}$ that contains only 0.8 mol % of Gd^{3+}. Second, it is clearly visible that a limit is rapidly reached with almost no further decrease of T_1 above 2.1 mol % of Gd^{3+}. These results are of importance in the frame of MRI applications as they show that limited amounts of Gd^{3+} may be used, which is of benefice when considering the toxicity of free Gd^{3+}.

MR-Imaging of MRI-PCLs. Having in hand MRI-PCLs with defined contents of gadolinium, we were interested in evaluating the influence of (i) the overall amount of gadolinium present in the samples and (ii) the grafting density of Gd^{3+} complexes immobilized on the PCL backbone on the MR visualization. The final aim was to evaluate the optimum compromise between MRI-visibility and low dose of Gd^{3+}. For this purpose, circular films (10 mg, 0.8 cm^2) of mixed PCL and MRI-PLCs ($\mathbf{4_1}$, $\mathbf{4_2}$, and $\mathbf{4_3}$) were prepared with increasing Gd^{3+} concentrations in the range 2−40 μg of Gd^{3+} per film. T_1 signal enhancement was compared to a PCL control film. One should note that films morphologies were not uniform, as a result of the film formation process, and PCLs mixtures presented different filming-properties. This nonuniformity may have an effect on T_1 enhancement as Gd^{3+}-based T_1 enhancement is mainly dependent on the inner sphere relaxation phenomenon which implies water molecules exchange at the Gd^{3+} site. However, in the present study this effect, if existing, was not preponderant as shown by the following results. First, it is noticeable that all Gd^{3+}-containing films presented a T_1 signal enhancement, whereas PCL films did not (Figures 4 and S7). At constant Gd^{3+} grafting density (rows in Figure 4), the signal enhancement increased with the overall content of Gd^{3+} for all copolymers, with an evident and clear signal observed above 2.5 μg of Gd^{3+} per mg of PCL. Indeed, irrespective of the grafting density, the signal enhancement was weak for lower doses, as seen for films 1−9 and strongly enhanced above 2.5 μg Gd^{3+} per mg of PCL as seen for films 10−15. Second, assessment of grafting density effect on MR conspicuity was done by considering a constant overall Gd^{3+} content (columns in Figures 4 and S7). Two behaviors were found. For low Gd^{3+} contents, below 2.5 μg of Gd^{3+} per mg of PCL, signal enhancement was improved with the copolymers $\mathbf{4_2}$ and $\mathbf{4_3}$ that presented high grafting densities (film 4 vs films 5 and 6 and film 7 vs films 8 and 9). This was not the case at higher Gd^{3+} contents, above 2.5 μg of Gd^{3+} per mg of PCL, with even a decrease of T_1 signal enhancement for the copolymers $\mathbf{4_2}$ and $\mathbf{4_3}$ compared to $\mathbf{4_1}$, as clearly shown by comparison between film 13 and films 14 and 15. This signal decrease is likely due to susceptibility effects resulting from high local Gd^{3+} concentrations.[35] These combined observations tend to demonstrate that a compromise between the two parameters, namely, the overall Gd^{3+} content and the Gd^{3+} grafting density on the polymer backbone, seems to be necessary for optimal MR visualization. This corroborates the evolution of T_1 relaxation times that showed that above 2.1 mol % no further T_1 decrease was observed. It also confirms the fact that a fine control of Gd^{3+} content and grafting density is of first importance for

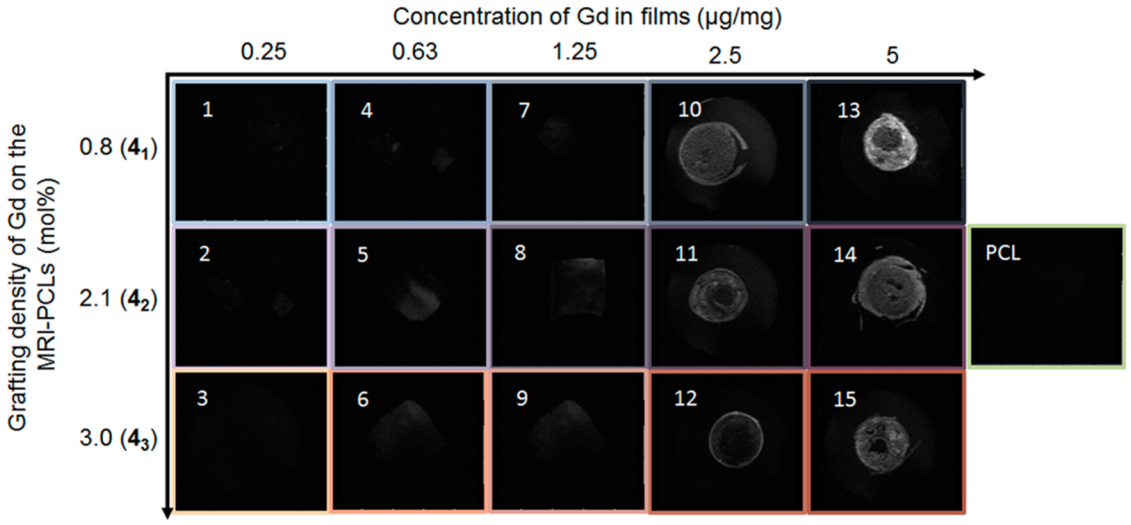

Figure 4. MR visualization of PCL/MRI-PCLs **4** films as a function of the total amount of Gd^{3+} per film and of the Gd^{3+} grafting density on the MRI-PCLs backbones.

dx.doi.org/10.1021/bm400978a | *Biomacromolecules* 2013, 14, 3626−3634

optimal MR visualization. In vivo implantations should now be planned to confirm our approach and thoroughly evaluate the benefit of MRI-visibility of MRI-PCLs.

Stability and Cytocompatibility of MRI-PCLs. *In Vitro Stability of MRI-PCLs.* Our aim being to provide long-term visualization through the use of hydrophobic and slow degrading copolyesters, we evaluated the in vitro stability of compounds **4** to detect any release of free Gd^{3+}, which has been associated with nephrogenic systemic fibrosis disorder (NFS).[36,37] Indeed, for long-term visualization and to avoid adverse effects in the body, it was important to determine whether any gadolinium salts were released from the MRI-PCLs. With regards to the removal of carboxylate groups, three left against five in Magnevist, one can postulate that the stability of the complex could be decreased with a higher dissociation constant (K_d) and, thus, a material that is less stable than an unmodified small molecule chelate. This was not the case for a DTPA/Gd^{3+}-PCL recently synthesized by our group, which had four carboxylate groups.[6,7] Given that compounds **4** are not water-soluble, whereas thermodynamic and kinetic constants are measured in aqueous solution, the stability of compounds **4** was studied by titrating by ICP-MS the Gd^{3+} released in aqueous medium. Results are shown in Figure 5. Release

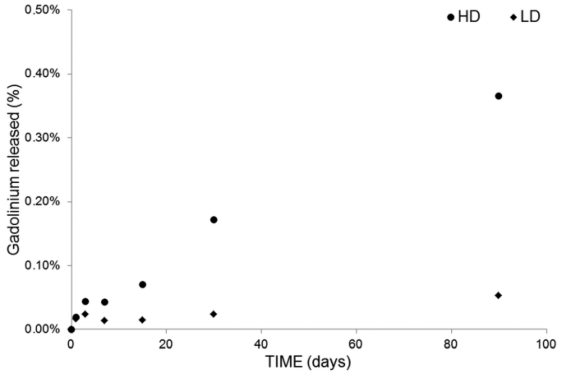

Figure 5. Stability study performed on mixed films of PCL and $\mathbf{4}_2$ having high dose (HD, 0.4 wt %) and low dose (LD, 0.1 wt %) of Gd^{3+} (PBS; 37 °C).

kinetics were run in PBS at 37 °C and over a 90 day period. The amount of released Gd^{3+} after 90 days was low whatever the initial content of gadolinium in the films. It was limited to a maximum concentration of released Gd^{3+} of 0.45 and 13 μg/L for LD and HD films, respectively (0.065 μg/L for PBS negative control). The corresponding cumulative percentages of released Gd^{3+} were therefore of 0.05% for the film containing 10 μg of Gd^{3+} (LD film) and 0.4% for the film containing 40 μg of Gd^{3+} (HD film). In addition, release profile in PBS showed a limited and steady release. Taking into account the linear portion of the curves, it was possible to extrapolate the period required to release 1% of the total Gd^{3+} amount under the used conditions. One year for HD films and six years for LD films were estimated. This result shows that, under the used conditions, the measured release is indeed not significant and that the PCL-based MMCAs can be considered as stable. Comprehensive explanation of the parameters explaining the observed stability despite a decreased number of a carboxylate available for Gd^{3+} complexation is beyond the scope of this work but the following could be considered: (i) ester groups in the polymer may possibly offset the loss of these carboxylate groups or (ii) perhaps the entropy of the system limits the Gd^{3+} dissociation. However, and to confirm this trend, future in vitro release study should be undertaken in more complex mediums like human serum or PBS completed with physiologically relevant concentrations of $ZnCl_2$ (0.03 wt %) and albumin (4 wt %) to evaluate the influence of proteins and cations on the MRI-PCLs complex stability.[38,39] One should also consider future in vivo implantation to evaluate the possible influence of enzymes, macrophages, and transient changes in pH (especially pH changes during inflammation) that may appear in vivo.

These results should be compared to the Gd^{3+} decomplexation after clinical injection of commercial Gd^{3+}-based contrast agents. Indeed, when dealing with Gd^{3+}-based contrast agents, the question usually arises of associated NFS in patients with renal failure. However, it is noteworthy that this phenomenon is usually observed after a conventional MR scan where patients receive 1.0−2.5 g Gd^{3+} as a bolus (posology of 0.1−0.2 mmol/kg of contrast agent for an intravenous injection of Magnevist).[40−42] In vitro studies performed in native serum at pH 7.4 and 37 °C showed an initial decomplexation rate of 0.16% per day,[43] which corresponds to 1.6−4 mg of circulating free Gd^{3+} before renal clearance. In the present work, a clear T_1 enhancement was observed for films loaded with 13 μg/cm^2 of Gd^{3+}. To compare with our previous results,[7] if used to coat a classical 10 × 10 cm implanted mesh for soft tissue prolapses, this would correspond to an overall dose of 2 mg of Gd^{3+}. One can note the similarity between this overall dose of immobilized Gd^{3+} and the extent of circulating free Gd^{3+} estimated for a clinical MR scan. Additionally, it is worth noting that, for a maximum release of 0.4%, as obtained in this work after 90 days, the maximal amount of free Gd^{3+} released by such a mesh would be 8 μg, which represents less than 0.5% of the circulating free Gd^{3+} during a conventional scan.

In Vitro Cytocompatibility of MRI-PCLs. An evaluation of murine fibroblast proliferation was performed on polymer films to assess the cytocompatibility of MRI-PCLs and determine whether they are suitable for cell culture and potential cell-contacting biomedical applications. Films containing 0.1 wt % of Gd^{3+} were prepared from compound $\mathbf{4}_2$ for this evaluation. Figure 6 shows the proliferation at 1, 2, and 3 days of L929 murine fibroblasts on MRI-PCL films compared to native PCL and TCPS. It may be concluded from this proliferation experiment that the surface of MRI-PCL did not impede fibroblast proliferation. In addition, this result tends to

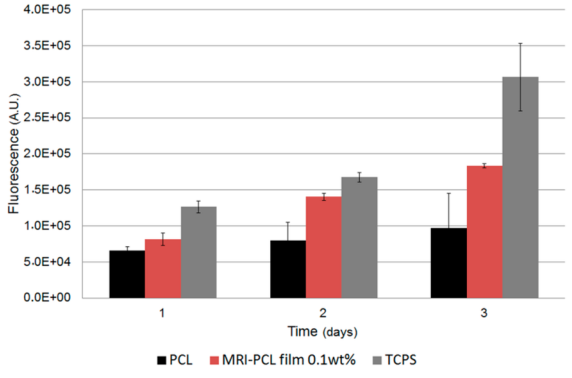

Figure 6. L929 proliferation on MRI-PCL films ($\mathbf{4}_2$, red) compared to TCPS (positive control, gray) and PCL films (black); data are expressed as mean ± SD and correspond to measurements in triplicate.

dx.doi.org/10.1021/bm400978a | *Biomacromolecules* 2013, 14, 3626−3634

demonstrate that the presence of free carboxylate on the polymer backbone was not dentrimental to cell proliferation although some of the free calcium present in the culture medium may be complexed. Indeed, this is not surprising considering the very low effective concentration of free ligand on the MRI-PCL. Typically, if one considers the amount of MRI-PCL used to coat a classical 10 × 10 cm implanted mesh for soft tissue prolapses, it represents a negligible 6 μmol of potential free ligand to be compared with the physiological concentration of calcium between 2.2 and 2.6 mM. Taking into account that PCL is widely recognized as a biocompatible material, MRI-PCLs would appear to be suitable for the growth of fibroblasts and cell-contacting applications.

CONCLUSION

In this work, we presented the efficient convergent synthesis of novel hydrophobic macromolecular agents based on poly(ϵ-caprolactone). PCLs with controlled propargyl group ratios yield MRI-PCLs with defined Gd^{3+} grafting densities. ^{1}H NMR, FT-IR, and ICP-MS analyses confirmed the efficient coupling of the complex on the PCL backbones via a main mechanism of intramolecular cross-linking that led to MRI-PCLs containing 1.0, 2.6, and 3.6 wt % of Gd^{3+}. T_1 relaxation times were highly impacted with a 70% reduction for grafting densities as low as 0.8 mol %. T_1 relaxation time measurements also showed that low grafting ratios were sufficient to obtain MRI-visible materials. No further influence is detectable for substitution ratios above 2.1 mol %. This was confirmed by the MR experiments with Gd^{3+}-containing films. All of them presented a T_1 signal enhancement and best results were obtained for films containing more than 2 μg of Gd^{3+} per mg of PCL. MR experiments also demonstrated the role of Gd^{3+} grafting density. A fine control and a compromise between the overall Gd^{3+} content and the Gd^{3+} grafting density on the polymer backbone is necessary for optimal MR visualization. These novel MMCAs have been found to be stable over a 90 day period with less than 0.5% of Gd^{3+} released in PBS. Finally, they also were found to be cytocompatible, with good proliferation of fibroblasts, which confirms the high potential of these novel hydrophobic PCL-based MMCAs for biomedical applications.

ASSOCIATED CONTENT

Supporting Information

^{1}H NMR spectrum of **1**, MTB test of **2** and **4**, ^{1}H NMR, FT-IR, and SEC analyses of **3**, and MR visualization of **4** with higher contrast. This material is available free of charge via the Internet at http://pubs.acs.org.

AUTHOR INFORMATION

Corresponding Author

*E-mail: benjamin.nottelet@univ-montp1.fr.

Notes

The authors declare no competing financial interest.

ACKNOWLEDGMENTS

The authors wish to thank the French Ministry of Education and Research for S.E.H.'s fellowship, the Erasmus program for B.P.'s fellowship, Chantal Douchet and Olivier Bruguier for ICP-MS analyses and Sylvie Hunger and Cedric Paniagua for NMR analyses.

REFERENCES

(1) Gallez, B.; Baudelet, C.; Jordan, B. F. *NMR Biomed.* **2004**, *17* (5), 240−262.
(2) Fischer, T.; Ladurner, R.; Gangkofer, A.; Mussack, T.; Reiser, M.; Lienemann, A. *Eur. Radiol.* **2007**, *17* (12), 3123−3129.
(3) Lapray, J. F.; Costa, P.; Delmas, V.; Haab, F. *Prog. Urol.* **2009**, *19* (13), 953−969.
(4) Birch, C. *Best Pract. Res. Clin. Obstet. Gynaecol.* **2005**, *19* (6), 979−991.
(5) Nottelet, B.; Coudane, J.; Vert, M. *Biomaterials* **2006**, *27* (28), 4948−4954.
(6) Blanquer, S.; Guillaume, O.; Letouzey, V.; Lemaire, L.; Franconi, F.; Paniagua, C.; Coudane, J.; Garric, X. *Acta Biomater.* **2012**, *8* (3), 1339−1347.
(7) Guillaume, O.; Blanquer, S.; Letouzey, V.; Cornille, A.; Huberlant, S.; Lemaire, L.; Franconi, F.; de Tayrac, R.; Coudane, J.; Garric, X. *Macromol. Biosci.* **2012**, *12* (10), 1364−1374.
(8) Aime, S.; Castelli, D. D.; Crich, S. G.; Gianolio, E.; Terreno, E. *Acc. Chem. Res.* **2009**, *42* (7), 822−831.
(9) Beilvert, A.; Cormode, D. P.; Chaubet, F.; Briley-Saebo, K. C.; Mani, V.; Mulder, W. J. M.; Vucic, E.; Toussaint, J. F.; Letourneur, D.; Fayad, Z. A. *Magn. Reson. Med.* **2009**, *62* (5), 1195−1201.
(10) Ladd, D. L.; Hollister, R.; Peng, X.; Wei, D.; Wu, G.; Delecki, D.; Snow, R. A.; Toner, J. L.; Kellar, K.; Eck, J.; Desai, V. C.; Raymond, G.; Kinter, L. B.; Desser, T. S.; Rubin, D. L. *Bioconjugate Chem.* **1999**, *10* (3), 361−370.
(11) Lee, H. Y.; Jee, H. W.; Seo, S. M.; Kwak, B. K.; Khang, G.; Cho, S. H. *Bioconjugate Chem.* **2006**, *17* (3), 700−706.
(12) Lucas, R. L.; Benjamin, M.; Reineke, T. M. *Bioconjugate Chem.* **2008**, *19* (1), 24−27.
(13) Shiraishi, K.; Kawano, K.; Minowa, T.; Maitani, Y.; Yokoyama, M. *J. Controlled Release* **2009**, *136* (1), 14−20.
(14) Toth, E.; Helm, L.; Kellar, K. E.; Merbach, A. E. *Chem.−Eur. J.* **1999**, *5* (4), 1202−1211.
(15) Vaccaro, M.; Accardo, A.; Tesauro, D.; Mangiapia, G.; Lof, D.; Schillen, K.; Soderman, O.; Morelli, G.; Paduano, L. *Langmuir* **2006**, *22* (15), 6635−6643.
(16) Zarabi, B.; Nan, A. J.; Zhuo, J. C.; Gullapalli, R.; Ghandehari, H. *Macromol. Biosci.* **2008**, *8* (8), 741−748.
(17) Zong, Y.; Guo, J.; Ke, T.; Mohs, A. M.; Parker, D. L.; Lu, Z. R. *J. Controlled Release* **2006**, *112* (3), 350−356.
(18) Fu, Y. J.; Raatschen, H. J.; Nitecki, D. E.; Wendland, M. F.; Novikov, V.; Fournier, L. S.; Cyran, C.; Rogut, V.; Shames, D. M.; Brasch, R. C. *Biomacromolecules* **2007**, *8* (5), 1519−1529.
(19) Grogna, M.; Cloots, R.; Luxen, A.; Jerome, C.; Passirani, C.; Lautram, N.; Desreux, J. F.; Detrembleur, C. *Polym. Chem.* **2010**, *1* (9), 1485−1490.
(20) Pressly, E. D.; Rossin, R.; Hagooly, A.; Fukukawa, K. I.; Messmore, B. W.; Welch, M. J.; Wooley, K. L.; Lamm, M. S.; Hule, R. A.; Pochan, D. J.; Hawker, C. J. *Biomacromolecules* **2007**, *8* (10), 3126−3134.
(21) Shokeen, M.; Pressly, E. D.; Hagooly, A.; Zheleznyak, A.; Ramos, N.; Fiamengo, A. L.; Welch, M. J.; Hawker, C. J.; Anderson, C. J. *ACS Nano* **2011**, *5* (2), 738−747.
(22) Zhang, G. D.; Zhang, R.; Wen, X. X.; Li, L.; Li, C. *Biomacromolecules* **2008**, *9* (1), 36−42.
(23) Franconi, F.; Roux, J.; Garric, X.; Lemaire, L. *Magn. Reson. Med.* **2013**, DOI: 10.1002/mrm.24666.
(24) Villaraza, A. J. L.; Bumb, A.; Brechbiel, M. W. *Chem. Rev.* **2010**, *110* (5), 2921−2959.
(25) Darcos, V.; El Habnouni, S.; Nottelet, B.; El Ghzaoui, A.; Coudane, J. *Polym. Chem.* **2010**, *1* (3), 280−282.
(26) Carboni, B.; Benalil, A.; Vaultier, M. *J. Org. Chem.* **1993**, *58* (14), 3736−3741.
(27) Perez-Baena, I.; Loinaz, I.; Padro, D.; Garcia, I.; Grande, H. J.; Odriozola, I. *J. Mater. Chem.* **2010**, *20* (33), 6916−6922.
(28) Brown, R.; Clarke, D. W.; Daffner, R. H. *Am. J. Roentgenol.* **2000**, *175*, 1087−1090.

(29) Vonarbourg, A.; Sapin, A.; Lemaire, L.; Franconi, F.; Menei, P.; Jallet, P.; Le Jeune, J. J. *Magn. Reson. Mater. Phys., Biol. Med.* **2004**, *17* (3−6), 133−139.
(30) Anelli, P. L.; Fedeli, F.; Gazzotti, O.; Lattuada, L.; Lux, G.; Rebasti, F. *Bioconjugate Chem.* **1999**, *10* (1), 137−140.
(31) Bryson, J. M.; Chu, W. J.; Lee, J. H.; Reineke, T. M. *Bioconjugate Chem.* **2008**, *19* (8), 1505−1509.
(32) Fernandez-Trillo, F.; Pacheco-Torres, J.; Correa, J.; Ballesteros, P.; Lopez-Larrubia, P.; Cerdan, S.; Riguera, R.; Fernandez-Megia, E. *Biomacromolecules* **2011**, *12* (8), 2902−2907.
(33) Parac-Vogt, T. N.; Kimpe, K.; Laurent, S.; Pierart, C.; Elst, L. V.; Muller, R. N.; Binnemans, K. *Eur. J. Inorg. Chem.* **2004**, *17*, 3538−3543.
(34) *Product Monograph: MAGNEVIST Gadopentetate Dimeglumine Injection*; Bayer Inc.: Toronto, Ontario, 2012; submission control No. 156553, pp 1−38.
(35) Villringer, A.; Rosen, B. R.; Belliveau, J. W.; Ackerman, J. L.; Lauffer, R. B.; Buxton, R. B.; Chao, Y. S.; Wedeen, V. J.; Brady, T. J. *Magn. Reson. Med.* **1988**, *6* (2), 164−174.
(36) Goulle, J. P.; Saussereau, E.; Mahieu, L.; Bouige, D.; Groenwont, S.; Guerbet, M.; Lacroix, C. *J. Anal. Toxicol.* **2009**, *33* (2), 92−98.
(37) Thakral, C.; Abraham, J. L. *Radiol. Clin.* **2009**, *47* (5), 841−853.
(38) Baranyai, Z.; Palinkas, Z.; Uggeri, F.; Brucher, E. *Eur. J. Inorg. Chem.* **2010**, *13*, 1948−1956.
(39) Laurent, S.; Elst, L. V.; Henrotte, V.; Muller, R. N. *Chem. Biodiversity* **2010**, *7* (12), 2846−2855.
(40) *VIDAL: le Dictionnaire*, 88th ed.; Vidal: Paris, 2012.
(41) Grobner, T. *Nephrol. Dial. Transpl.* **2006**, *21* (4), 1104−1108.
(42) Idee, J. M.; Port, M.; Raynal, I.; Schaefer, M.; Le Greneur, S.; Corot, C. *Fund. Clin. Pharmacol.* **2006**, *20* (6), 563−576.
(43) Frenzel, T.; Lengsfeld, P.; Schirmer, H.; Hutter, J.; Weinmann, H. J. *Invest. Radiol.* **2008**, *43* (12), 817−828.